Magnetic and structural characterization of ultra-thin Fe (222) films

Melissa G. Loving, Emily E. Brown, Nicholas D. Rizzo, and Thomas F. Ambrose

Citation: AIP Advances **8**, 056108 (2018);
View online: https://doi.org/10.1063/1.5006444
View Table of Contents: http://aip.scitation.org/toc/adv/8/5
Published by the American Institute of Physics

Magnetic and structural characterization of ultra-thin Fe (222) films

Melissa G. Loving,[a] Emily E. Brown, Nicholas D. Rizzo,
and Thomas F. Ambrose
Northrop Grumman Corporation, 1212 Winterson Road, Linthicum, MD 21090, USA

(Presented 7 November 2017; received 25 September 2017; accepted 28 October 2017;
published online 14 December 2017)

Varied thickness body centered cubic (BCC) ultrathin Fe films (10-50Å) have been sputter deposited onto Si (111) substrates. BCC Fe with the novel (222) texture was obtained by H- terminating the Si (111) starting substrate then immediately depositing the magnetic films. Structural results derived from grazing incidence x-ray diffraction and x-ray reflectivity confirm the crystallographic texture, film thickness, and interface roughness. Magnetic results indicate that Fe (222) exhibits soft magnetic switching (easy axis), high anisotropy (hard axis), which is maintained across the thickness range, and a positive magnetostriction (for the thicker film layers). The observed soft magnetic switching in this system makes it an ideal candidate for future magnetic memory development as well as other microelectronics applications that utilize magnetic materials. https://doi.org/10.1063/1.5006444

I. INTRODUCTION

Elemental Fe exhibits a rich body of crystallographic and magnetic phases which may be achieved through variations in extrinsic parameters. Conventionally, body centered cubic (BCC) Fe is a soft ferromagnetic material with a <100> easy axis of magnetization.[1] To date, a majority of spintronic related studies have been conducted on thin films with the (100) out-of-plane orientation. Thus, it is worthwhile to explore Fe films with other crystallographic orientations for integration into multilayer magnetic stacks. Previous work has shown that body centered cubic (BCC) Fe (222) may be achieved when Fe is deposited onto a H_2 terminated Si surface.[2] Further, it is well-established that ultrathin films (<100Å thickness) can have properties that differ substantially from their bulk counterparts. To this end, we provide a fundamental examination of the structural and magnetic properties of ultrathin BCC (222)-oriented Fe films, with a [222] principle crystallographic easy axis of magnetization. The observed soft ferromagnetic switching in Fe (222) makes this system particularly desirable as a candidate for magnetic memory applications, which require small, reproducible switching fields and minimal defects.

II. EXPERIMENTAL

A BCC phase of ultrathin Fe (nominal thickness ranges from 10-50Å) has been sputter deposited onto six inch Si (111) substrates. Prior to Fe deposition, the Si (111) surface was H_2-terminated in order to achieve the novel (222) texturing. H-termination of the starting Si (111) surface was achieved by rinsing the front of the wafer with a concentrated 49% HF solution for 30 seconds, immediately before deposition; this approach is an adaptation of previously published work.[2] The Fe films were deposited in an applied field from a single target (>99.9% purity). Deposition was done at ambient

[a]Corresponding author: Melissa.Loving@ngc.com

temperature with an argon sputter gas, base pressure of $<3x10^{-8}$ torr, and a DC power of 500W, which yields a growth rate of ~0.5 Å/s, as calibrated by *ex-situ* X-ray reflectivity (XRR) measurements (data not provided here). Following Fe deposition the films were capped with 100Å Nb (BCC) in order to prevent oxidation of the Fe film layers.

The film layer thickness and crystal structure were confirmed using x-ray scattering techniques on a 6 circle BedeD1 diffractometer. The film crystal structure was probed using grazing incidence x-ray diffraction (GI-XRD). The room temperature GI-XRD measurements were made with a fixed ω angle of ω = 2° and the resultant diffraction patterns were indexed to a Fe BCC unit cell. Low angle, specular XRR measurements were made on the films to confirm film thicknesses of the individual layers and examine compositional grading through the film interfaces. The resultant XRR patterns were fit using the Jordan Valley Refs simulation software.

Room temperature magnetic measurements were made on an SHB Looper (Mesa600). In general, the SHB Looper uses inductive pickup coils to measure magnetic flux to produce a magnetic flux (B) *vs.* field (H) measurement. The SHB Looper also has the capability to measure the magnetostrictive effect in samples by utilizing the inverse magnetostriction effect. Specifically, the SHB Looper measures changes in anisotropy field (H_k), due to applied mechanical strain. The determination of H_k follows this general procedure: 1) estimate the slope of the transition region of the hard axis loop, 2) extrapolate the slope to the intersection of the previously measured B_s value 3) report H_k as the horizontal intersection point. The slope of the transition region is determined by defining two points and measuring the slope between these points. The location of the two points is specified by their horizontal coordinates; that is, these points in the transition region will have a vertical coordinate of ½ B_s. The change in H_k (ΔH_k) between mechanically unstressed and stressed samples is an indirect measure of magnetostriction and can be correlated to a magnetostriction coefficient (λ) *via* the following relationship:

$$\lambda \sim \Delta H_k \cdot M_s/(E \cdot \varepsilon) \quad (1)$$

Where M_s is the saturation magnetization, E is the Young's modulus, and ε is the film strain. Details on this measurement, measurement setup and subsequent calculations can be found in the literature referenced here.[3,4]

III. RESULTS AND DISCUSSION

Figure 1(a)–(b) shows the representative GI-XRD and XRR results of the 50Å Fe film. Here, only the (110) reflection of Nb (2θ = 38.474°) can be seen as the Bragg reflection for Fe (222) occurs at 2θ = 137.136°, which is outside of the 2θ arm hardware limit for the x-ray detector system used here (2θ motor arm limit is 2θ = 120°). The attainment of Fe (222) is therefore inferred from an absence of the characteristic Bragg reflections corresponding to (110) Fe (2θ = 44.673°) or (200) Fe (2θ = 65.021°). Further, there is no evidence for a (111) Fe reflection arising from an FCC Fe

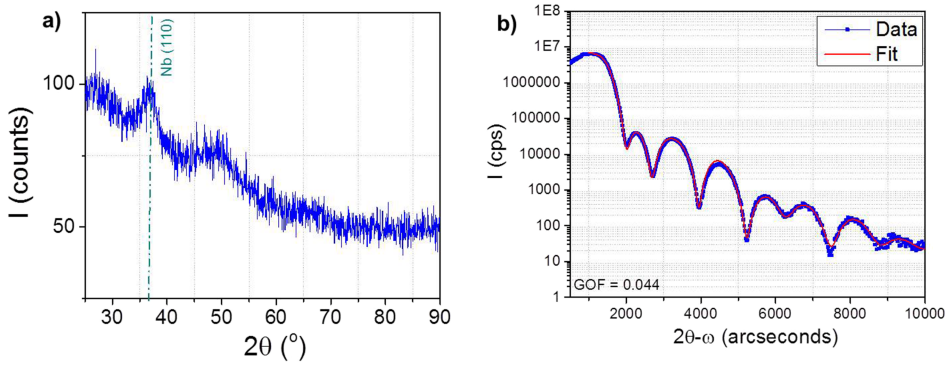

FIG. 1. a) GI-XRD and b) XRR patterns of a 50Å thick Fe film. From the GI-XRD only a (110) reflection from the Nb cap is evident suggesting the attainment of (222) Fe, the remainder of the background features are attributed to the Si (111) substrate (i.e. features observed at 2θ = 28° and 2θ = 47°).

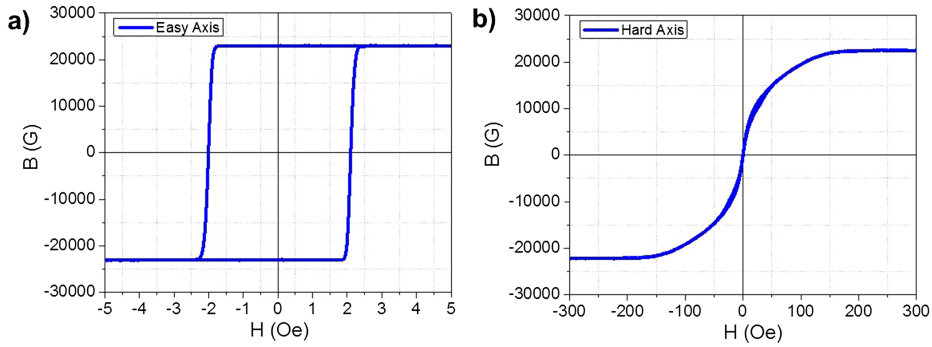

FIG. 2. Magnetic induction (B) *vs*. field (H) loops of a 50Å (222) Fe film where a) corresponds to easy axis magnetization and b) corresponds to hard axis magnetization.

phase (2θ = 42.758). It should also be noted that BCC Fe (222) was also inferred from a 500Å thick Fe film; in this sample neither the film thickness nor the beam intensity were factors that may contribute to a lack of observed Bragg reflections (data not shown here). Figure 1(b) shows the XRR pattern and simulation model of the film stack architecture. Here, the goodness of fit (GOF) of the displayed simulation was 0.044 (where GOF = 0 is a perfect fit). These XRR fits assumed an infinite Si substrate layer, NbO_x passivation layer (40Å), metallic Nb layer (60Å), metallic Fe layer, and a $FeSi_x$ layer. From the XRR fits, the $FeSi_x$ layer (at the Si (111)/Fe interface) makes up ~30% of the total Fe film layer and was observed through the entirety of the Fe thickness series, described in this manuscript.

Figure 2 shows representative easy and hard axis switching character of the 50Å Fe film layer (at T = 300 K). The easy axis of this film shows soft ferromagnetic character while the hard axis

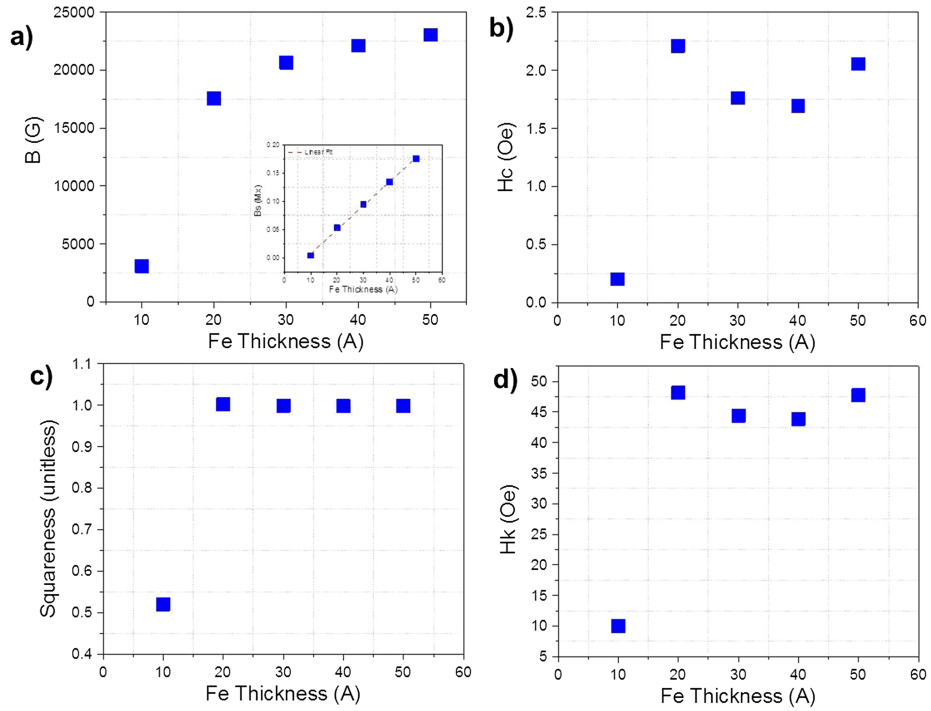

FIG. 3. Thickness trend plots of ultrathin (222) Fe films for a) magnetic induction (B) b) Easy axis coercivity (H_c) c) easy axis squareness and d) hard axis anisotropy field (H_k). Inset of a) shows linear fit to raw B_s values to obtain a magnetic dead layer thickness of 8.11Å.

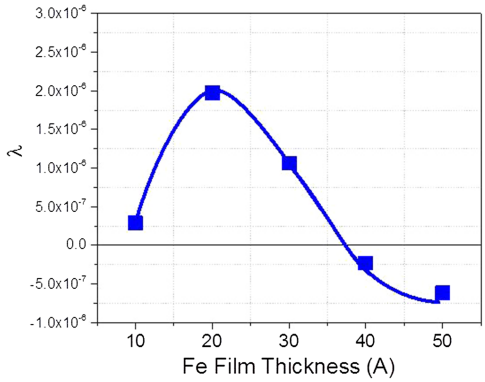

FIG. 4. Dependence of magnetostriction (λ) on (222) Fe film thickness.

exhibits a large anisotropy field. Similar data were collected for the 40, 30, 20 and 10Å thick Fe films ($B(H)$ loops not included here). Here, the anisotropy field can be considered an indirect indicator of the crystal anisotropy that holds the magnetization oriented in the easy direction. That is, the large anisotropy field observed in Fe (222) indicates strong crystal anisotropy along the Fe [222] direction. The trend plots for the saturation value of the magnetic induction (B_s), easy axis coercivity (H_c) and squareness (defined as the ratio between the magnetic remanence and the magnetic saturation), and hard axis anisotropy field (H_k) are shown in Figure 3(a)–(d). From Figure 3(a) (inset), a magnetic dead layer (nonmagnetic portion of the as-deposited Fe film layers) can be determined as the x-intercept of a linear fit to the B_s values *vs.* film thickness. The magnetic dead layer for the films described here is calculated to be 8.11Å, which indicates that films deposited at a thickness of 8.11Å or less are anticipated to be nonmagnetic at room temperature. This large magnetic dead layer may be attributed to the large $FeSi_x$ component (~30%) which was observed in the XRR fits (Figure 1(b)). The magnetic easy axis H_c, squareness, and hard axis H_k values appear to be nominally constant at thicknesses ≥20 Å. The drop in these magnetic parameters at the Fe film thickness of ≤10Å is attributed to the large portion of the film which is considered nonmagnetic (~80% of the total relative film thickness).

Finally, Figure 4 shows the calculated magnetostriction values for this series as a function of the Fe film thicknesses. The values obtained here of the magnetostriction of the ultrathin Fe films are lower than what is expected for bulk Fe (*i.e.* $\lambda_{100} = +21\times10^{-6}$ or $\lambda_{111} = -21\times10^{-6}$),[5] but are comparable to thin film forms of (100) Fe and (110) Fe (*i.e* $\lambda = 5\rightarrow-5\times10^{-6}$).[6] From Figure 4, a thickness dependence of the magnetostriction values can also be noted. The positive magnetostriction values suggest that when the Fe is magnetized in the [222] direction, the length of the crystal increases, alternatively, the negative magnetostriction values suggest a reduction in the crystal length. The shift in the striction from positive to negative, suggests that there may be a shift in the internal stress of the films with the increased film thickness.

IV. CONCLUSIONS

Here, ultrathin (222)-oriented Fe films (BCC) have been synthesized and characterized structurally and magnetically. It has been demonstrated that, in a (222) orientation ultrathin Fe films can produce a near-ideal soft ferromagnetic response (low coercivity, high squareness, high anisotropy). Further, this system shows a significant reduction in magnetostriction values, as compared to bulk Fe, while still maintaining a positive magnetostriction value. These features make this system interesting for the incorporation of magnetic thin films into functional microelectronics devices as well as a test-bed for providing basic insight into the complexities between structure and properties of thin film systems.

[1] B. D. Cullity and C. D. Graham, *Introduction to Magnetic Materials*, Hoboken: John Wiley & Sons, Inc., 2009.
[2] J. Ye, W. He, Q. Wu, H.-L. Liu, X.-Q. Zhang, Z.-Y. Chen, and Z.-H. Cheng, "Determination of magnetic anisotropy constants in Fe ultrathin film on vicinal Si(111) by anisotropic magnetoresistance," Scientific Reports **21**, 1–6 (2013).

[3] A. C. Tam and H. Schroeder, "Precise measurements of a magnetostriction coefficient of a thin soft-magnetic film deposited on a substrate," Journal of Applied Physics **64**(10), 5422–5424 (1988).
[4] L. Baril, B. Gurney, and D. S. V. Wilhoit, "Magnetostriction in spin valves," Journal of Applied Physics **85**(8), 5139–5141 (1999).
[5] S. Chikazumi, *Physics of Magnetism* (Robert E. Krieger Publishing Company, Inc., Malabar, FL, 1964).
[6] N. Ishiwata, C. Wakabayashi, and T. Matsumoto, "Zero magnetostriction in iron films," IEEE Transactions on Magnetics **24**(6), 3078–3080 (1988).